

PAPER • **OPEN ACCESS**

Tritium-titanium target degradation due to deuterium irradiation for DT neutron production

To cite this article: M. Rajput *et al* 2023 *Nucl. Fusion* **63** 066033

View the [article online](#) for updates and enhancements.

You may also like

- [An Algorithm for Target Tracking of the Car in Accident](#)
Siyuan Zhang, Yunqing Liu and Yile Dai
- [Small target detection and window adaptive tracking based on continuous frame images in visible light background](#)
Zheng Wang, Jianping Zeng, Xiaoli Xie et al.
- [Numerical Simulation Study of Target Response under Underwater Explosion](#)
Jiabao Peng and Feng Ma

Tritium-titanium target degradation due to deuterium irradiation for DT neutron production

M. Rajput^{1,3,*}, H.L. Swami¹, S. Vala^{1,2}, M. Abhangi^{1,2}, Ratnesh Kumar¹ and R. Kumar^{1,2}

¹ Institute for Plasma Research, Gandhinagar 382428, India

² Homi Bhabha National Institute, Anushaktinagar 400094, India

E-mail: mmayankrajput@outlook.com

Received 24 April 2022, revised 11 January 2023

Accepted for publication 17 April 2023

Published 12 May 2023



Abstract

In the present article, we have investigated tritium removal from tritium-titanium targets during fusion neutron production and the impact of tritium degradation on neutron production. The removal of tritium from the target is predicted for deuterium ion irradiation with the SDTrimSp code. We adopt the binary collision approximation method to simulate the recoils and projectile trajectories and concentration of constituents in the target. We have modelled four phenomena in our simulations; ion exchange, sputtering, outgassing of tritium, and thermal diffusion of hydrogen isotopes in the target caused by deuterium irradiation. Insignificant contributors such as burn-up of tritium in neutron production and loss of tritium due to radioactive decay are not included in our model. This tritium removal results in the nonuniform distribution of tritium in the target. A Python-based script is developed to investigate the effects of tritium removal on neutron production with these pristine and irradiated targets. This script uses the layered composition of the constituents' atoms, DT reaction cross-section, and stopping power of deuterium ions in the target. The script is validated with the NeuSdesc code for the pristine target. Using the layered composition of tritium atoms in the target obtained from the SDTrimSp simulations, the script predicts the degradation in neutron production for different irradiation scenarios.

Keywords: DT neutrons, deuterium irradiation, tritium removal, neutron yield calculations

(Some figures may appear in colour only in the online journal)

1. Introduction

Nuclear fusion energy is one of the possible alternative energy sources to conventional coal and gas operated power plants and has the potential to provide carbon-free energy in the

near future. The huge potential availability of primary fuel for future developments, relatively short-lived radioactive waste, no actinides production, and no runaway reaction are some of the advantages associated with fusion energy [1]. Primary fuels for fusion energy are deuterium and tritium. Deuterium can be extracted from sea water and tritium can be bred from the ${}^6\text{Li}(n, {}^3\text{H}){}^4\text{He}$ and ${}^7\text{Li}(n, {}^3\text{H} + n){}^4\text{He}$ reactions. One major concern associated with fusion reactors is the handling of 14.1 MeV energy neutrons. These neutrons are capable of producing gases, radioactive isotopes, and causing displacement damage [2, 3], thus affecting the lifetime and functionality of fusion reactor components [4]. From the neutronics point of view, the prime requirements for the successful realisation of fusion power are to have accurate and precise nuclear data for

³ Present address: Tokamak Energy, Milton Park, Abingdon, United Kingdom of Great Britain and Northern Ireland.

* Author to whom any correspondence should be addressed.



Original content from this work may be used under the terms of the [Creative Commons Attribution 4.0 licence](https://creativecommons.org/licenses/by/4.0/). Any further distribution of this work must maintain attribution to the author(s) and the title of the work, journal citation and DOI.

the materials to be used in it [5], to understand the effects of fusion neutrons on reactor components including electronics and structural materials [6] and to investigate tritium breeding capabilities of breeder blankets [7]. The validation of evaluated nuclear cross-section data, investigation of the effects of 14.1 MeV energy neutrons on the fusion reactor components, and tritium breeding capabilities of various breeding blankets require the 14.1 MeV neutron sources at laboratories [8, 9]. These 14.1 MeV neutrons are also very useful in medical radioisotope production, fundamental nuclear physics experiments, fast neutron detector development, and neutron imaging tool developments [10–12]. Tritium-titanium targets are among such commercially available targets [13–16] that are used to produce the 14.1 MeV energy neutrons through the ${}^2\text{H}({}^3\text{H},n){}^4\text{He}$ reaction at various laboratories [9, 10, 17, 18]. The interactions of deuterium ions with the tritium-titanium target remove tritium via sputtering, outgassing, diffusion, replacement with deuterium ions, or ion exchange while some fraction of tritium is utilized in the neutron production [19]. Tritium loss due to sputtering, outgassing, and ion exchange affects neutron production and governs the target lifetime. The estimation of tritium removal is also important in radiation safety during neutron production.

In the present work, we have investigated the tritium-titanium target degradation with time due to deuterium ion irradiation. The investigation involves the following steps;

1. We have computationally modelled the sputtering, outgassing, ion exchange, and tritium diffusion in the tritium-titanium targets and predicted tritium removal from target due to the deuterium ion irradiation at different energies.
2. We have developed a Python-based script to predict the neutron yield from the pristine and irradiated target.
3. We have investigated the degradation in neutron production with increasing deuterium fluence at different energies and suggested the best irradiation scenario for the maximum utilization of the target.

This manuscript is structured as follows; section 2 presents the methodology and simulation details, section 3 presents the results of tritium removal, change in the concentration of tritium at a different depth, section 4 presents the development of a script to predict the neutron spectra, and prediction of lifetime of tritium-titanium target, and section 5 presents the conclusion of this article.

2. Methodology and simulation details

The gaseous compounds of hydrogen isotopes e.g. hydrogen, deuterium, and tritium gas have characteristics of disassociating and dissolving in their atomic form on metal surfaces. The atoms of these isotopes recombine on the surface and start permeating through the metal depth. Titanium has high hydrogen retention, absorption, and storage characteristics and due to these, it is often used as a base material for hydrogen, deuterium, and tritium storage and Copper is used as a substrate [13]. Tritium loading in the titanium metal is carried out either with electron gun evaporation or with the thermal evaporation

methods [13]. The evaporation temperature, the ratio of tritium and titanium atoms, surface area and thickness of titanium metal govern the properties of tritium titanium target and tritium activity associated with it [20, 21]. In this manuscript, we have modelled the commercially produced tritium target from manufacturers such as SODERN, etc [13]. The mass density of TiT_2 target is taken to be 4.09 g cm^{-3} [22] which corresponds to the atomic density of $1.387 \times 10^{23} \text{ atoms cm}^{-3}$.

The processes that govern the tritium depletion in the target are sputtering, ion exchange, diffusion, outgassing, radioactive decay, and consumption in neutron production. If N_{Trit} is the number of tritium atoms in the layers of target and the target is irradiated with fluence ϕ with the interval of $d\phi$, then the change in the concentration of tritium atoms in each layer can be represented as;

$$\frac{dN_{\text{Trit}}}{d\phi} = -[N_{\text{Trit}}(\text{sputtered}) + N_{\text{Trit}}(\text{ion exchange}) + N_{\text{Trit}}(\text{outgassed}) + N_{\text{Trit}}(\text{decayed}) + N_{\text{Trit}}(\text{utilized}) + N_{\text{Trit}}(\text{diffusion})] \quad (1)$$

This sputtering process removes tritium and titanium atoms from the surface during the bombardment of deuterium ions. Deuterium ions share the same chemical and material properties similar to tritium, thus replacing the atoms of tritium. This ion exchange process ends up depleting the tritium atoms near the projected range of the deuterium ions [19, 23]. Deuterium and tritium have low binding energies in the metals, and if the maximum storage of these hydrogen isotopes is exceeded in any layer at higher fluence, atoms higher than the permissible limit are removed [24]. This phenomenon limits the number of hydrogen isotopes in each layer and depends on the number of atoms of titanium. The maximum loading limit for hydrogen isotopes is 2 in titanium. As both the hydrogen isotopes share similar chemical properties, both are removed in the same proportion. This phenomenon is referred to as outgassing in this manuscript. The ion irradiation causes swelling in the target, resulting in pressure arising in the target and it initiates a local transport of gas atoms. This local transport of gases causes the deuterium to transport into deeper depths and remove tritium even after their end range [25]. Tritium decays into helium-3 with a half-life of 12.3 years. When deuterium ions hit the tritium-titanium target, some deuterium ions react with the tritium and produce neutrons. The utilization rate or burn-up rate of tritium is very low compared to ion exchange and outgassing. For example, the utilization rate of tritium atoms is about 1.5×10^{-5} neutrons/deuterium ion for 135 keV energy deuterium beam [19]. We have not considered the burn-up of tritium and loss of tritium due to radioactive decay in the simulations. The deuterium and tritium also thermally diffuse in the target due to the density gradient [24].

In the present work, we have carried out the ion transport simulation with the SDTrimSP code (Version 6) [23]. The SDTrimSP code uses the binary collision approximation (BCA) method to simulate the interactions between projectile and target atoms [26]. The SDTrimSP code has been previously used for ion beam irradiation, deposition simulations, ion-induced damage, and ion beam modification in the targets

Table 1. Parameters used in the SDTrimSP code for BCA simulations.

Sr. no.	Parameter	Model
1	Surface binding model	Composition dependant surface binding energy
2	Interaction potentials	Ziegler–Biersack–Littmark (ZBL) [24]
3	Maximum atomic fraction of hydrogen isotopes in titanium	0.667
4	Inelastic energy loss model for deuterium, and tritium atoms	Ziegler–Biersack [33]
5	Inelastic energy loss model for copper and titanium	Lindhard–Scharff [34]
6	Thermal diffusion parameters for deuterium and titanium	$1.43 \times 10^{-5} \text{ m}^2 \text{ s}^{-1}$ [35]
7	Activation energy for deuterium and tritium	0.60 eV [35]
8	Temperature	300 K

[23, 25, 27–32]. The code simulates the ion deposition, sputtering, outgassing, and thermal diffusion of the atoms involved in the simulations. The SDTrimSP has two modes namely static and dynamics. In the static mode, the target composition remains fixed and in the dynamics mode, its composition, thickness, and density change due to sputtering, diffusion, and removal of atoms. We have carried out these simulations in dynamic mode. The parameters that we have used in our simulations are given in table 1.

These BCA simulations have been carried out in step irradiation of up to 10^{22} particles·cm⁻². Target details are given as;

- Target diameter = 3.8 cm, Tritium to Titanium ratio = 1.8, Tritium atomic fraction = 64.2857%, Titanium atom fraction = 35.725%, Atomic density = 1.387×10^{23} atoms cm⁻³, Mass density = 4.09 g cm⁻³, copper plate thickness = 1 mm.

The target is divided into 110 layers. The first 100 layers of tritium-titanium are 420 Å each followed by the 10 layers of copper backing of 1000 000 Å thickness each. The SDTrimSP code provides information of the atomic density and composition of each layer at each irradiation step. The number of hydrogen isotopes that exceed twice the atoms of titanium is corrected in each layer at every irradiation step and additional deuterium and tritium atoms are removed and considered as outgassed tritium and deuterium.

Due to tritium removal, the concentration of tritium gets reduced at a certain depth. This reduction of tritium results in reduced neutron yield. The neutron yield from tritium-titanium targets is simulated with the NeuSDesc code [36]. The NeuSDesc code calculates neutron yield from tritium targets using the two-body kinematics by assuming a uniform concentration of tritium in the target. It is not possible to incorporate the non-uniform concentration of tritium in the NeuSDesc code thus it cannot be used to predict the neutron yield from the irradiated target. In the present work, we have developed a Python-based script to predict neutron production from the irradiated target. This script has an advantage over NeuSDesc that the non-uniform tritium concentration of the target can be used with the script. This advantage allows us to use this script for the irradiated target. The script uses the DD and DT cross-section data from the ENDF-VIII cross-section data library [8] and has been validated with the NeuSDesc code for the pristine target. The details and flowchart of the script have been given

in section 4. The script is later used to predict the degradation in neutron production during irradiation.

3. Results and discussion

3.1. Range of ions and energy deposition of incident ions in the tritium target

The ion beam interacts with the tritium-titanium target and deposits its energy to electrons and atomic nuclei. The ion beam interactions with the matter are governed by the elastic energy transfer to nuclei, inelastic energy transfer to electrons, and exchange of energy between nuclei and electrons via electron-phonon coupling, and result in ion beam deposition, ionization, and atomic diffusion in the matter [37, 38]. The energy transfer to the nuclei results in atomic displacements and phonon energy dissipation for the energy higher than threshold damage energy (E_d) and lower than E_d , respectively. We present the projected range of deuterium ions of different energy and their energy deposition in the tritium-titanium target in figure 1. The target details have been provided in section 2. These simulations have been carried out with the SRIM code [23]. The SRIM code also uses the same ZBL universal interaction potentials and Biersack method to solve the scattering integral similar to SDTrimSP [23]. The SDTrimSP has additional capabilities of performing dynamic simulations, investigating the effects of stoichiometry changes due to the ion beam deposition and atomic mixing, and can also work on parallel computers. It is observed from figure 1 that a deuterium beam of above 800 keV energy cannot deposit its full energy to the target of 5.20 μm thickness, hence will remain underutilized. The stopping power of ions decreases with the increase in their energy, thus, to utilize the tritium-titanium target to its full extent, the projected range of the deuterium needs to be less than that of the thickness of the target. We have also observed that the neutron yield from the target increases up to 800 keV; after that the neutron yield starts decreasing with the increase of deuterium ion energy. We discuss this observation in section 4. The rest of the ion transport simulations have been carried out with the SDTrimSP code.

3.2. Tritium and titanium removal from target and change in the content of tritium in the target layers for different energy deuterium ions

In this work, we have modelled the ion sputtering, deuterium ion exchange, outgassing of hydrogen isotopes, and thermal

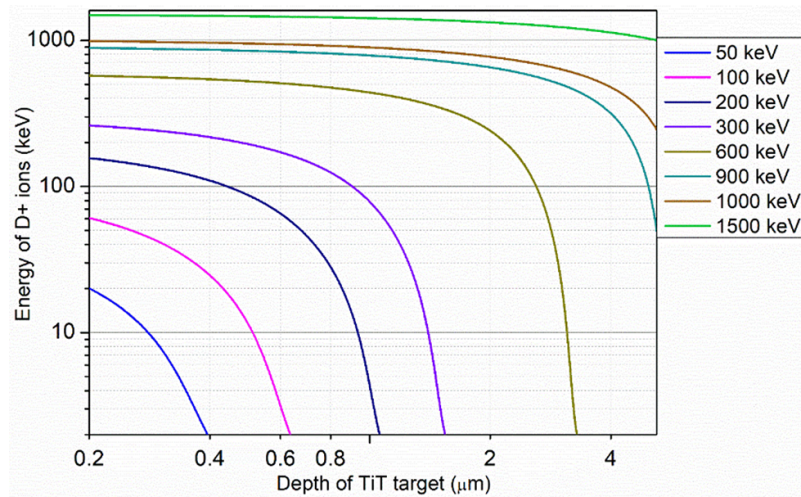


Figure 1. Energy loss of deuterium ions of different energies in the tritium-titanium target. X axis presents the remaining energy of deuterium ions (initial energy—energy loss).

diffusion of constituents in the target. The deuterium ions sputter out some fraction of tritium and titanium atoms from the near surface region and low energy ion sputters more tritium or titanium atoms. Due to the ion exchange process, deuterium atoms replace the tritium atoms near their end range and tritium is depleted from these regions. When the amount of hydrogen isotopes is exceeded in any layer over the permissible limit, the exceeded amount is removed via outgassing. The outgassing phenomenon starts removing tritium at higher ion irradiation levels ($\sim 1.5 \times 10^{18}$ ion irradiation). Thermal diffusion process causes the diffusion of deuterium ions from their end range, detrapping of tritium from its bound sites, and replacing tritium with deuterium [39]. Thermal diffusion cause tritium removal far from the end range to the end of the target depth. These simulations have been carried out at 300 K temperature. The maximum retained atomic fraction of both tritium and deuterium atoms is 66.67% in titanium [40]. Due to ion irradiation, the concentration of constituents of the target changes. We calculated the number of deuterium and tritium atoms at each irradiation step and then calculate the removed tritium and deuterium due to outgassing. We present the tritium removal due to ion exchange, sputtering, outgassing, and thermal diffusion from the target irradiated with the 300 keV deuterium ion in figure 2. Deuterium ion exchange is the dominant process that removes the tritium and the outgassing phenomenon starts removing tritium after 1.5×10^{18} deuterium fluence. Thermal diffusion causes diffusion of tritium atoms from their end range and removes tritium from a depth higher than their end range via ion exchange. It does not directly remove the tritium but enhances the tritium removal after a certain fluence level which is 2×10^{19} in the case of 300 keV deuterium ions. Initially at lower fluence, sputtering and deuterium ion exchange are the phenomenon that causes the removal of tritium but with increasing fluence, the outgassing phenomenon starts causing the tritium removal from the target. The beam current is 20 mA in these calculations. We present the results of tritium removal from the target for deuterium ions of different

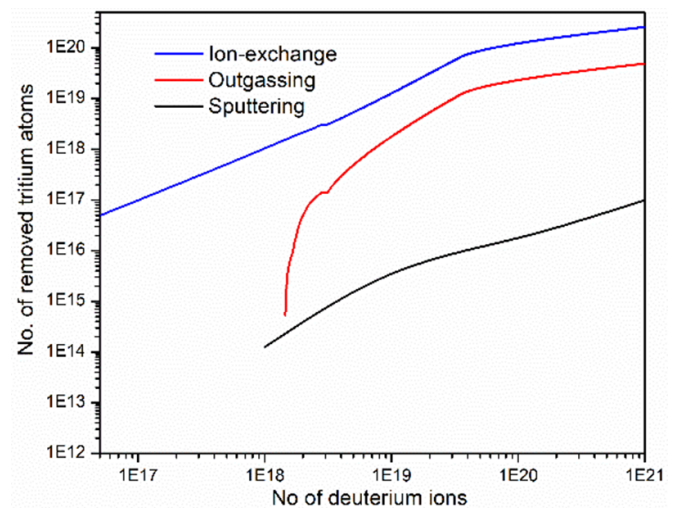


Figure 2. Tritium removal due to sputtering, outgassing and ion exchange phenomenon for the 300 keV deuterium ion irradiation energy. The X-axis and Y-axis represent the number of removed tritium atoms and irradiated deuterium ions on the target.

energies for the irradiation of up to 10^{21} particles·cm⁻² in figure 3.

It is observed that tritium removal is not uniform in the target. Initially, at the lower fluence level, deuterium ions are deposited near to projected range. For example, 300 keV deuterium ions have an end range of $\approx 1.7 \mu\text{m}$ in the pristine sample, thus at lower ion irradiation, it only removed tritium at their end range, but due to the continuous irradiation, thermal diffusion causes deuterium to diffuse from their end range and enhancing the tritium removal at depths higher than their end range. We present the concentration of tritium atoms at different depths for continuous irradiation of 300 keV deuterium ions for up to 10^{21} in figure 4.

A similar trend is observed for the 150 and 600 keV deuterium ion irradiation. We present the tritium concentration for different energy deuterium ions at 10^{21} deuterium ions in

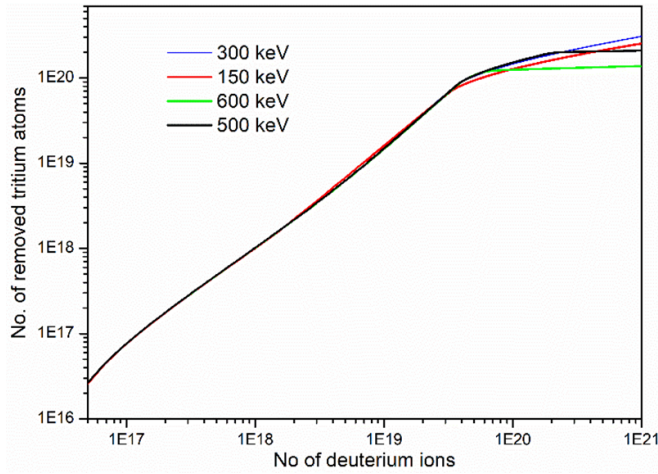


Figure 3. Tritium removal due to deuterium ion irradiation at different energies.

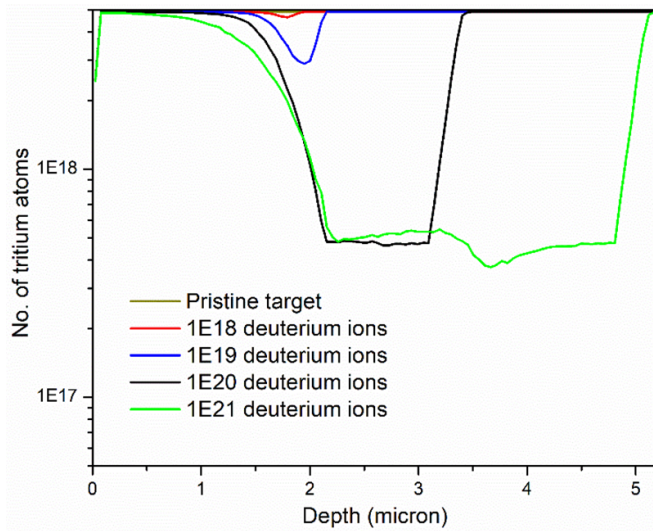


Figure 4. Concentration of tritium at depth for different irradiation levels of 300 keV deuterium ion irradiation.

figure 5. The tritium concentration at various depths was simulated at different energies for up to 10^{22} deuterium- cm^{-2} . This depth profile of tritium is further used to predict the performance of the target in neutron production and is discussed in the next section.

4. Development of a script to predict neutron spectra

The performance of the tritium-titanium target depends on the tritium concentration and energy of deuterium ions. Their degradation in neutron production is very important to predict as these neutrons are used to investigate fusion material research and validate the fusion benchmark and cross-section measurement experiments [19]. The NeuSdesc is one of the codes that is extensively used to predict the neutron spectra from the tritium-titanium targets [36]. It solves the two-body kinematics reaction to predict the neutron yield. As discussed

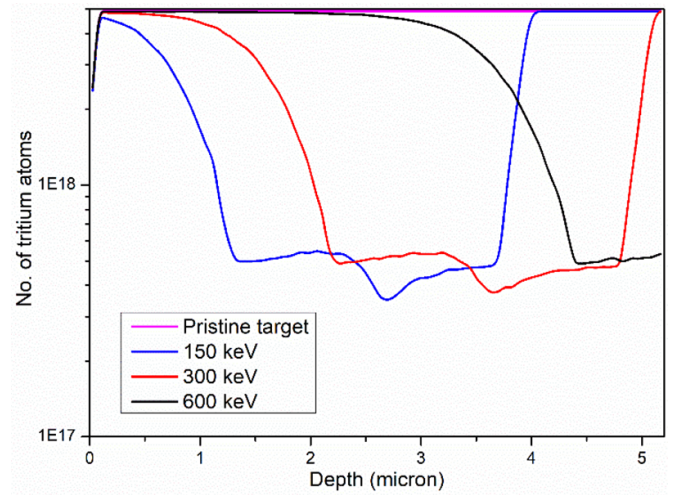


Figure 5. Depth profile of tritium concentration for different energies for 1×10^{21} deuterium ions.

earlier in this work, the tritium concentration does not remain uniform after irradiation, thus the NeuSdesc code cannot be used to investigate the performance of the irradiated target. To study the target performance with increasing deuterium ion irradiation, we have developed a Python-based script to predict the neutron spectra from the tritium-titanium target. The flowchart of the script is given in figure 6.

The steps involved in this flowchart are explained as;

1. We provide the target details. The details include the depth, atomic density, and number of deuterium, titanium, and tritium atoms in each layer of the target. The SDTrimSp code provides information on tritium atoms at each irradiation step.
2. The energy loss of deuterium ions is estimated in each layer. The stopping power data is taken from the SRIM [38].
3. We use the nuclear cross-section data of DD and DT reactions from the ENDF-VIII database [8].
4. Based on the energy of deuterium ions in each layer, and its respective cross-section, neutron yield is calculated in each layer until the energy of deuterium ions becomes zero. The energy and angular spectra of the neutrons can also be calculated.
5. The SDEF card to be used as source spectra in neutron transport code e.g. MCNP can also be calculated with this script.

This script can also calculate the anisotropy in the neutron spectrum and angular distribution of neutrons with the 2-body kinematics equations. The prediction of the script is validated with the NeuSdesc code for a pristine target and the results of the script and NeuSdesc code are presented in figure 7. The neutron yield is calculated for the target specified in section 2 and deuterium beam of 20 mA current. The results calculated with the script are in very good agreement with NeuSdesc's predictions.

It is observed that the production of neutrons inside the target is not uniform. The production of neutrons is governed by

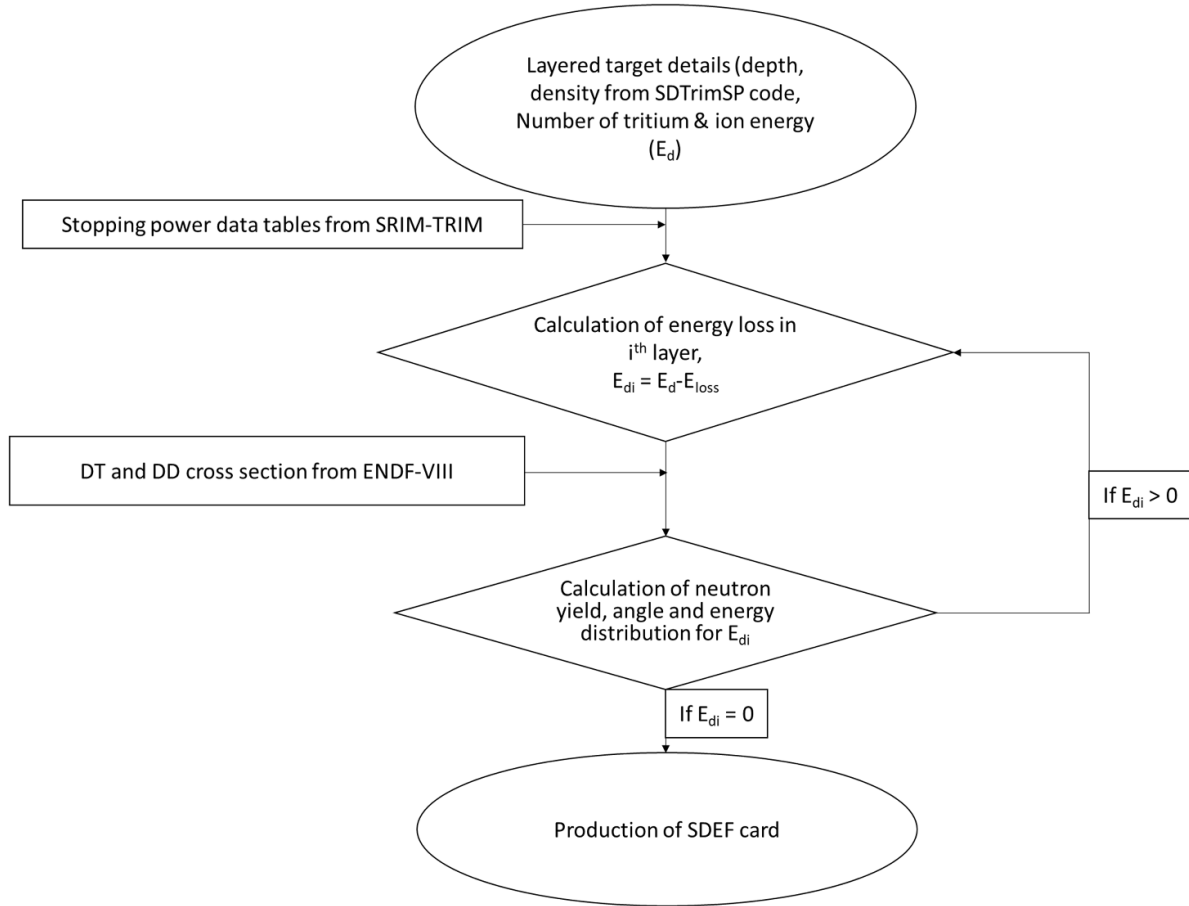


Figure 6. Flowchart of the Python-based script.

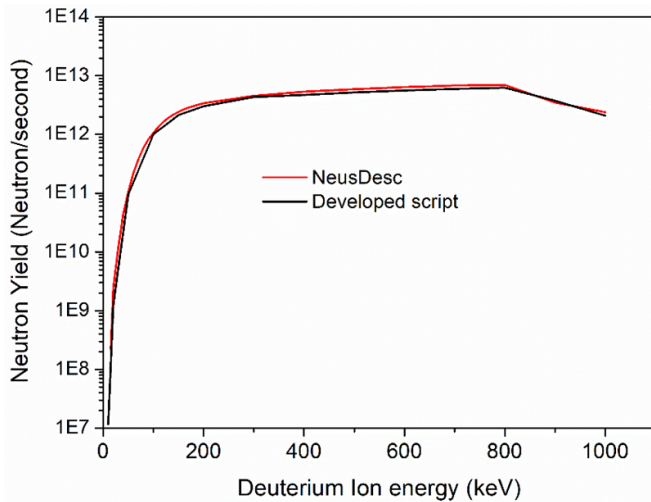


Figure 7. Prediction of neutron yield from the developed script and NeuSdesc code for 20 mA deuterium beam current.

the tritium concentration, available energy of the deuterium beam, and the cross-section of the DT reaction [41]. The cross-section peaks at around 110 keV energy, thus the depth at which the deuterium ion energy remains close to 110 keV

energy produces maximum neutrons. We present the depth profile of neutron production for 150, 300, 600, and 800 keV energy in figure 8. The higher energy deuterium ions utilize the innermost atoms effectively but the tritium atoms near the surface remain underutilized. In the next section, we use this script to predict the neutron production for the irradiated target.

4.1. Tritium target performance for successive deuterium irradiation

As discussed in the irradiation removes the tritium and titanium atoms from the target, thus also decreasing the density of the target at different depths. We have calculated the neutron production at different deuterium fluences for 300 keV and presented the results in figure 9. Figure 9 presents the depth distribution of neutron production at different irradiation fluences. As discussed earlier in section 2, the number of tritium atoms is decreased due to deuterium ions irradiation, which results in a decreased yield. The neutron production decreases with the increase of deuterium ion irradiation. As the deuterium fluences increase, a greater number of tritium atoms are removed from certain depths. With the increasing deuterium fluence, the neutron production yield

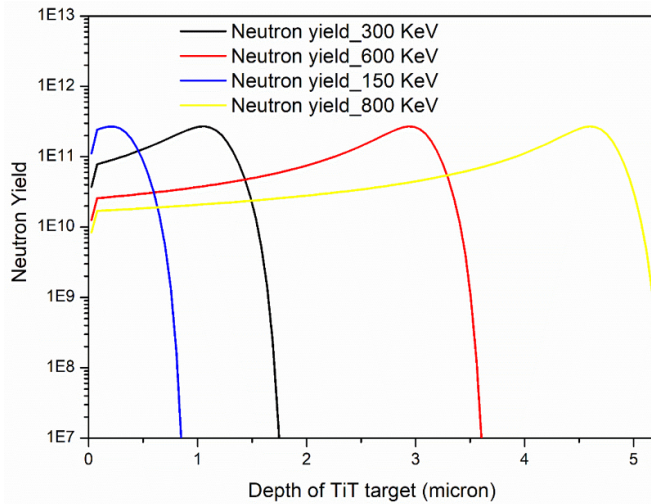


Figure 8. Neutron distribution at various depths in the tritium titanium target for 20 mA deuterium beam current at different energy deuterium ions.

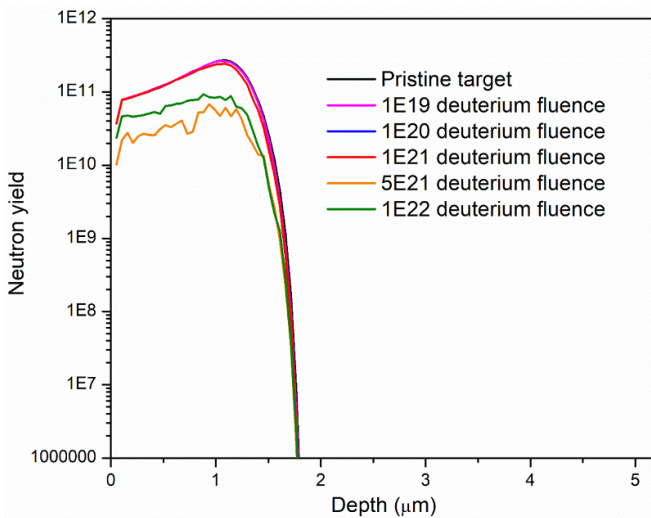


Figure 9. Neutron production after deuterium irradiation of different fluences for 300 keV energy.

reduces, and this degradation does not follow the same pattern for all the energies. The degradation in neutron production with time is presented in figure 10 for the deuterium ion beam of 20 mA. It is observed from the neutron yield prediction that target performance is better for the higher energies e.g. 300 and 600 keV. The performance of the target starts decreasing after 2×10^{17} deuterium fluence for 150 keV energy and its performance reduces to 10% at 10^{22} deuterium fluence. For 300 and 600 keV deuterium ions, target performance starts decreasing after 1×10^{19} deuterium fluence and its performance becomes $\sim 22\%$ and $\sim 25\%$ for 300 and 600 keV, respectively. These results recommend that the target should be used at higher deuterium ion energies to maximise its utilization and effective neutron production.

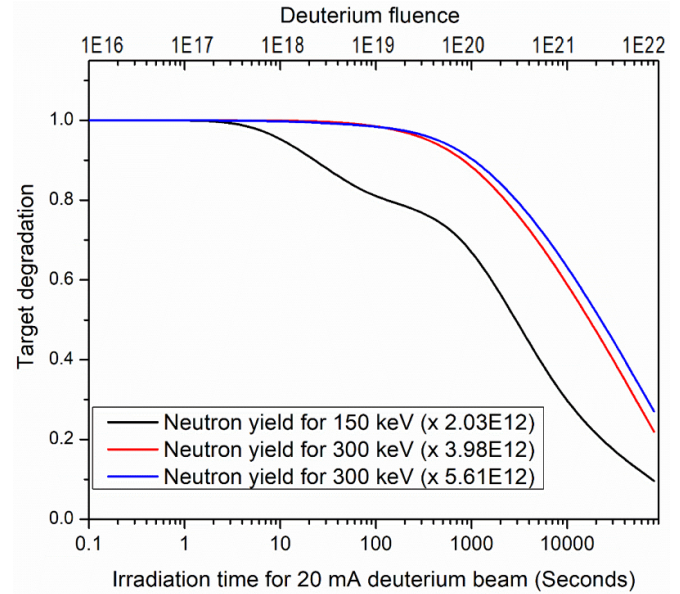


Figure 10. Performance of target with the increasing deuterium fluence.

5. Conclusion

This article can be divided into two parts; the first is the tritium removal from the tritium-titanium target and the second is the development of a script to predict the neutron yield from the pristine and irradiated targets. The first part presents an approach to predict the tritium removal from the tritium-titanium target during deuterium irradiation. The approach includes the modelling of four phenomena; ion exchange, sputtering, outgassing, and thermal diffusion of constituents' atoms in the target. The ion transport simulations in the target predict the range of deuterium ions of different energies in the target of $LR = 1.8$ and $5.20 \mu\text{m}$ thickness. The deuterium ions of up to 800 keV energy are fully absorbed in the target and thus will be fully utilized. The contributing phenomenon to the tritium removal is investigated and it is concluded that the ion exchange is the dominant phenomenon. The outgassing phenomenon starts removing tritium when the LR of the hydrogen isotopes in the target exceeds 2 and the LR exceeds 2×10^{19} particles for the 300 keV deuterium ion beam. Thermal diffusion causes tritium to diffuse from the end range of deuterium ions and enhances tritium removal. This approach is used to simulate the removal of tritium from the target for 150, 300, and 600 keV deuterium ion energy and provide the depth distribution of tritium in the target. The second part of this paper presents the development of a script to predict the neutron yield from the pristine and irradiation target. The script is developed with Python and validated with the NeuSdesc code. The script can provide the depth distribution of neutrons produced from the target irradiated with different deuterium ion energies. The results from the script show that the neutron yield increases up to 800 keV energy and afterwards it starts

decreasing. The script is used to predict the change in neutron production with increasing deuterium irradiation and to compare the performance of the target for different deuterium ion energies. The higher energy deuterium beam is more suitable for the higher yield neutrons for a longer period of deuterium irradiation. With the 150, 300 and 600 keV deuterium ion beam, the target can produce a neutron yield of more than 10^{12} neutrons·s⁻¹ for up to 10^{21} deuterium fluence. This deuterium fluence is equivalent to the 4.41 h of operation for the deuterium beam of 20 mA current. However, the 300 keV deuterium ion beam being used in most DT neutron generators can produce a continuous yield of $\sim 10^{12}$ neutrons·s⁻¹ for up to 2×10^{21} fluence, and at 1×10^{22} fluence, it can produce a neutron yield of $\sim 7.9 \times 10^{11}$ neutrons·s⁻¹.

References

- [1] Cowley S.C. 2016 The quest for fusion power *Nat. Phys.* **12** 384–6
- [2] Rajput M., Vala S., Subhash P.V., Srinivasan R., Kumar R. and Abhangi M. 2018 Primary knock on atom spectra, gas production and displacement cross section for tungsten and chromium irradiated with neutrons at energies up to 14.1 MeV *Fusion Eng. Des.* **130** 114–21
- [3] Rajput M. and Srinivasan R. 2020 Study of transmutation, gas production, and displacement damage in chromium for fusion neutron spectrum *Ann. Nucl. Energy* **138** 107187
- [4] Rajput M. et al 2022 Deuterium ion irradiation impact on the current-carrying capacity of DI-BSCCO superconducting tape *Nucl. Energy Technol.* **54** 2586–91
- [5] Vilkhivskaya O. and Gilbert M. 2020 Nuclear data V&V analysis for fusion applications: integral Benchmarks and decay data *EPJ Web Conf.* **247** 10015
- [6] Rubel M. 2019 Fusion neutrons: tritium breeding and impact on wall materials and components of diagnostic systems *J. Fusion Energy* **38** 315–29
- [7] Swami H.L., Sharma D., Mistry A.N., Danani C., Chaudhuri P. and Srinivasan R. 2021 Helium cooled dual breeder blanket—preliminary design analyses of a candidate breeding blanket concept for near term Indian DEMO fusion reactor *Int. J. Energy Res.* **45** 11735–44
- [8] Brown D.A. et al 2018 ENDF/B-VIII.0: the 8th major release of the nuclear reaction data library with CIELO-project cross sections, new standards and thermal scattering data *Nucl. Data Sheets* **148** 1–142
- [9] Pietropaolo A., Andreoli F., Angelone M., Vetrella U.B., Fiore S., Loreti S., Pagano G., Pilotti R. and Pillon M. 2018 The Frascati Neutron Generator: a multipurpose facility for physics and engineering *J. Phys.: Conf. Ser.* **1021** 012004
- [10] Pudjorahardjo D.S., Wahyono P.I. and Syarip S. 2020 Compact neutron generator as external neutron source of subcritical assembly for Mo-99 production (SAMOP) *AIP Conf. Proc.* **2296**
- [11] Williams D.L., Brown C.M., Tong D., Sulyman A. and Gary C.K. 2020 A fast neutron radiography system using a high yield portable DT neutron source *J. Imaging* **6** 128
- [12] Grimes S.M., Haight R.C., Alvar K.R., Barschall H.H. and Borchers R.R. 1979 *Phys. Rev. C* **16** 2127–37
- [13] Bach P. et al 2001 Tritium target manufacturing for use in accelerators *AIP Conf. Proc.* **576** 1141
- [14] Vala S., Abhangi M., Kumar R., Sarkar B. and Bandyopadhyay M. 2017 Rotating tritium target for intense 14-MeV neutron source *Fusion Eng. Des.* **123** 77–81
- [15] Sumita K. 1989 Tritium solid targets for intense D-T neutron production and the related problems *Nucl. Instrum. Methods Phys. Res. A* **282** 345–53
- [16] Booth R. and Barschall H.H. 1972 Tritium target for intense neutron source *Nucl. Instrum. Methods* **99** 1–4
- [17] Vala S.J., Abhangi M., Kumar R., Tiwari S., Kumar R., Swami H.L. and Bandyopadhyay M. 2020 Development and performance of a 14-MeV neutron generator *Nucl. Instrum. Methods Phys. Res. A* **959** 163495
- [18] Knaster J. et al 2017 *Nucl. Fusion* **57** 102016
- [19] Wampler W.R., Doyle B.L., Vizkelethy G., Bielejec E.S., Snow C.S., Styron J.D. and Jasica M.J. 2019 *14 MeV DT Neutron Test Facility at the Sandia Lon Beam Laboratory* (Albuquerque, NM: Sandia National Laboratories)
- [20] Causey R.A., Karnesky R.A. and San Marchi C. 2012 Tritium barriers and tritium diffusion in fusion reactors *Compr. Nucl. Mater.* **4** 511–49
- [21] Wang T., Grambole D., Grötzschel R., Herrmann F., Kreißig U., Eichhorn F., Brauer G. and Möller W. 2002 Mobility and retention of implanted hydrogen in Ti225 titanium alloy *Surf. Coat. Technol.* **158–159** 139–45
- [22] Csikai J.G. 1987 *Handbook of Fast Neutron Generators* vol I (Boca Raton, FL: CRC Press)
- [23] Hofsäss H., Zhang K. and Mutzke A. 2014 Simulation of ion beam sputtering with SDTrimSP, TRIDYN and SRIM *Appl. Surf. Sci.* **310** 134–41
- [24] Mutzke A.G., Schneider R., Eckstein W., Dohmen R., Schmid K., von Toussaint U and Badelow G. 2019 SDTrimSP version 6.00 IPP 2019–02 (Garching Max-Planck-Institut für Plasmaphysik)
- [25] Mutzke A., Rai A., Schneider R., Angelin E.J. and Hippler R. 2012 Modeling of altered layer formation during reactive ion etching of GaAs *Appl. Surf. Sci.* **263** 626–32
- [26] Demange G., Antoshchenkova E., Hayoun M., Lunéville L. and Simeone D. 2017 Simulating the ballistic effects of ion irradiation in the binary collision approximation: a first step toward the ion mixing framework *J. Nucl. Mater.* **486** 26–33
- [27] Mutzke A. and Eckstein W. 2008 Ion fluence dependence of the Si sputtering yield by noble gas ion bombardment *Nucl. Instrum. Methods Phys. Res. B* **266** 872–6
- [28] Rai A., Mutzke A. and Schneider R. 2010 Modeling of chemical erosion of graphite due to hydrogen by inclusion of chemical reactions in SDTrimSP *Nucl. Instrum. Methods Phys. Res. B* **268** 2639–48
- [29] Wittmaack K. and Mutzke A. 2012 Depth of origin of sputtered atoms: exploring the dependence on relevant target properties to identify the correlation with low-energy ranges *Nucl. Instrum. Methods Phys. Res. B* **281** 37–44
- [30] Wittmaack K. and Mutzke A. 2017 Highly accurate nuclear and electronic stopping cross sections derived using Monte Carlo simulations to reproduce measured range data *J. Appl. Phys.* **121** 105104
- [31] Mutzke A., Bandelow G. and Schneider R. 2015 Sputtering of mixed materials of beryllium and tungsten by hydrogen and helium *J. Nucl. Mater.* **467** 413–7
- [32] Lu Y. and Zhang P. 2013 First-principles study of temperature-dependent diffusion coefficients: hydrogen, deuterium, and tritium in α -Ti *J. Appl. Phys.* **113** 193502
- [33] Ziegler J.F., Ziegler M.D. and Biersack J.P. 2010 SRIM—the stopping and range of ions in matter *Nucl. Instrum. Methods Phys. Res. B* **268** 1818–23
- [34] Lindhard J. and So A.H. 1996 Relativistic theory of stopping for heavy ions *Phys. Rev. A* **53** 2443–56
- [35] Wipf H., Kappesser B. and Werner R. 2000 Hydrogen diffusion in titanium and zirconium hydrides *J. Alloys Compd.* **310** 190–5

- [36] Lövestam G. and Birhersson E. 2008 *NeuSDesc neutron source description software manual* LA-NA-23794-EN-C Institute for Reference Materials and Measurements (Joint Research Centre) (<https://doi.org/10.2787/10970>)
- [37] Zhang Y. and Weber W.J. 2020 Ion irradiation and modification: the role of coupled electronic and nuclear energy dissipation and subsequent nonequilibrium processes in materials *Appl. Phys. Rev.* **7** 041307
- [38] Weber W.J. and Zhang Y. 2019 Predicting damage production in monoatomic and multi-elemental targets using stopping and range of ions in matter code: challenges and recommendations *Curr. Opin. Solid State Mater. Sci.* **23** 100757
- [39] Hughey B.J. 1995 A long-lived tritiated titanium target for fast neutron production *Nucl. Instrum. Methods Phys. Res. B* **95** 393–401
- [40] Hueng L.K. 1994 *Titanium for Long-Term Tritium Storage* (Westinghouse Savannah River Company)
- [41] Bosch H.S. and Hale G.M. 1992 Improved formulas for fusion cross-sections and thermal reactivities *Nucl. Fusion* **32** 611–31